Identification of a human synaptotagmin-1 mutation that perturbs synaptic vesicle cycling

Baker et al (2015)

Index to Supplemental Data

Legend to Supplemental Video 1

Movie was recorded by the proband's parents during a typical period of night-time activity, and has been edited to illustrate his symptoms and impairments:

(A) Rapid involuntary limb movements.

(B) Involuntary vocalisation.

(C) Left lower limb dystonia, left hand dystonia.

(D) Upper limb and lower limb chorea; transitions between lying and sitting.

(E) Lower limb ballismus; rolling and pulling to stand.

(F) Dystonia and chorea whilst mobilising with support.

(G) Mixed hyperkinetic abnormalities during and after transition from standing to sitting.

Supplemental Figure 1 - <u>EEG spectral analysis</u>

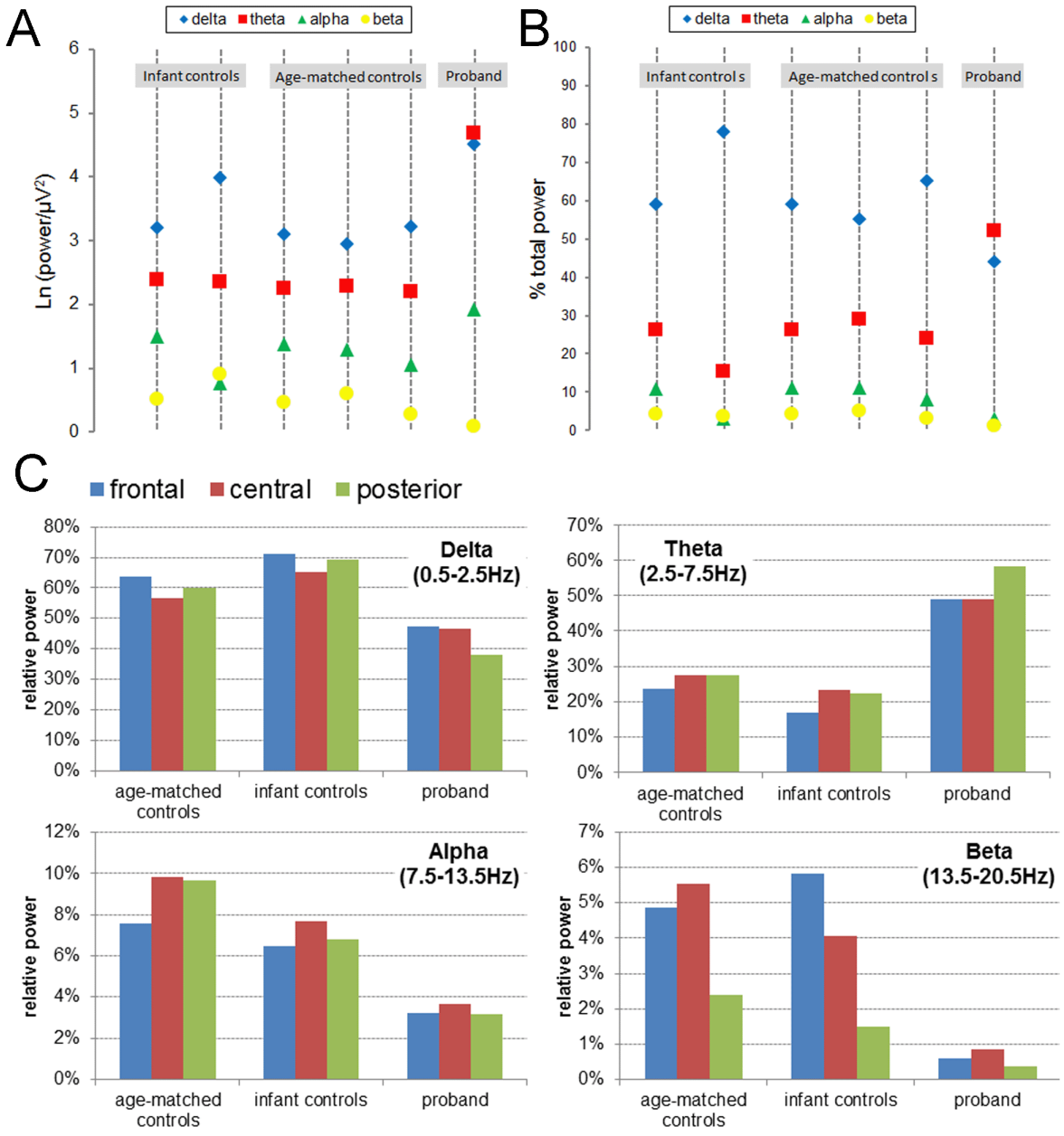

(A) EEG power (absolute) averaged across all electrodes. In comparison to age-matched and infant healthy controls, the proband demonstrates increased power within the delta frequency range, but maximally increased power within the theta frequency range. (B) EEG power (relative) averaged across all electrodes. The contributions of alpha and delta activity to total power are reduced whilst the contribution of theta activity to total power is approximately doubled for the proband in comparison to healthy controls. (C) Regional distribution of activity within different frequency ranges does not differ markedly between the proband and age-matched or infant controls. Frequency band definitions according to Clarke et al (2001).

Supplemental Figure 2 – <u>Auditory Evoked Potentials</u>

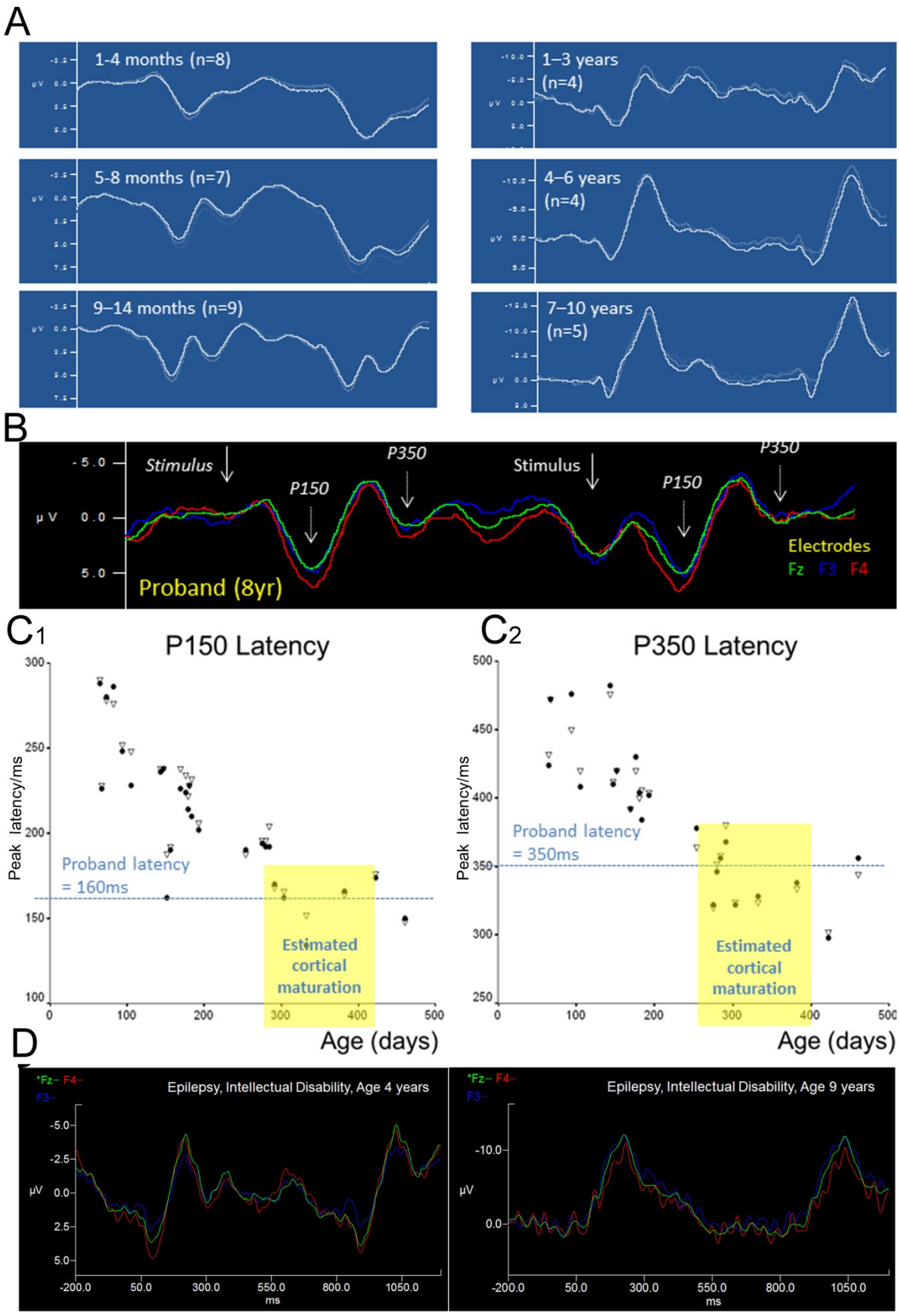

(A) Time-locked AEP to a 50ms 600Hz pure tone stimulus (interstimulus interval 700ms), averaged across all artefact-free trials for 9-14 month old healthy infants. (B) AEP for the proband, demonstrating similar morphology and amplitude to 9-14 month old healthy controls. (C) Cortical maturational age for the proband is estimated as 300-400 days, extrapolating from AEP latency trajectories in healthy controls (triangles = electrode F3, circles = electrode F4). (D) AEPs in two individual subjects with epilepsy and intellectual disability (secondary to Sturge Weber Syndrome).

Supplemental Table 1 - Rare de novo variants identified in the proband

Chromosome	Position[a]	rsNCBI ID	Reference allele	Alternative allele	Gene	Variant type	cDNA	Protein	Amino acid change
7	128766794	.	T	C	.	Within non-coding gene	.	.	-
7	144060802	rs145771593	C	T	*ARHGEF5*	Non-synonymous coding	1214	347	T|I
9	71849286	.	TTTTCTTT CTTTCTTT CTTTCTTT CTTTCTTT	TTTTCTTT CTTTCTTT CTTTCTTT CTTTCTTT CTTT	*TJP2*	Intronic	.	.	-
12	79842738	.	T	C	*SYT1*	Non-synonymous coding	1774	368	I|T
19	53122138	rs35821944	G	A	*ZNF83*	Intronic	.	.	-
19	53122146	rs35489438	A	C	*ZNF83*	Intronic	.	.	-
19	53122155	rs35672405	A	C	*ZNF83*	Intronic	.	.	-
19	55324635	rs649216	T	C	*KIR2DL4*	Synonymous coding	756	252	F
22	22974940	rs57741889	T	C	*POM121L1P*	3-prime UTR	3081	.	-

[a] HG19

Supplemental Methods

Clinical Investigations

Haematological and biochemical investigations were normal including white cell enzymes, plasma urate, carnitines, ammonia, transferrins, purines, pyrimidines, trace elements and urine organic acids. CSF investigations were normal including glucose, protein, lactate, neopterin, methyltetrahydrofolate, tetrahydrobiopterin, dihydrobiopterin, homovanillic acid and 5-hydroxyindoleacetic acid. Chromosomal investigations were normal at 4 Mb resolution by G-banded karyotype and at 200kb by comparative genomic hybridisation using Agilent custom 2x105K(v.2) oligoarray. Candidate gene investigations (*FMR1, UBE3A, ARX*) identified no mutations.

Neurophysiology protocols

EEG was acquired within a hospital setting by expert paediatric neurophysiologist, using silver/silver chloride electrodes arranged according to the International 10-20 system. Ground electrode was placed on the forehead and horizontal EOG recorded from the outer canthus of the left and right eyes. The recording system had gain of 566016, A/D sampling rate of 1000 Hz, band pass of .05-100 Hz, and a notch filter at 50 Hz. Resistance at each electrode was kept below 10 kW.

Spectral analysis was carried out in comparison to three healthy children aged 7 to 8 years of age (age-matched controls), and two healthy infants aged 7 months and 1 year of age (infant controls), using the same recording equipment and analysis protocol. Continuous EEG recordings were obtained for between 7 and 20 minutes and non-overlapping epochs (2048 data points) were created with random onsets through the recording after masking for obvious movement artefacts. 274 epochs were available for analysis for the proband, and number of epochs for comparison subjects ranged from 132 to 333. Mean signal power across all epochs within frequency bands was extracted according to Clarke et al (1). Regional distribution was analysed by averaging relative band powers across frontal (Fp1, Fp2, Fz, F3, F4), central (C3, C4, Cz, T7, T8) and posterior (P3, P4, Pz, Oz) electrodes.

Visual evoked potentials (VEPs) were recorded from posterior midline electrodes using a flash paired-pulse protocol (2). Paired-pulse flash VEPs were measured using interpulse intervals of 100, 200 and 500ms, with a repetition rate 1/s, bandwidth 1Hz. Findings were compared to flash VEP for a healthy age-matched child (tested at repetition rate 2/s). Numbers of averages were 256 for the proband and 128 for the healthy control.

Auditory event-related potentials (AEPs) were recorded in response to free-field presentation of pure tone stimuli of duration 50ms, frequency 600Hz, stimulus onset asynchrony 700ms. Continuous EEG was analysed offline using Neuroscan software version 4.3. Recordings were re-referenced to average reference. Band pass filtering (0.5-70Hz) was applied prior to manual rejection for movement-related artefacts, blink artefact reduction and automatic artefact rejection using +/-150μV amplitude criterion. Stimulus-locked epochs of 1200ms length (pre-stimulus baseline 200ms) were averaged for each subject for subsequent analysis. Trial numbers accepted for analysis after artefact rejection were comparable between the proband (223 trials accepted) and age-matched controls. AEP latencies were assessed in relation to developmental data collected from healthy infants using the same equipment and protocol (3).

Exome sequencing and bioinformatics

DNA (1-3μg) was sheared to 100-400 bp using a Covaris E210 or LE220 (Covaris, Woburn, MA, USA). Sheared DNA was subjected to Illumina paired-end DNA library preparation and enriched for target sequences (Agilent Technologies; Human All Exon 50 Mb - ELID S02972011) according to manufacturer's recommendations (Agilent Technologies; SureSelectXT Automated Target Enrichment for Illumina Paired-End Multiplexed Sequencing). Enriched libraries were sequenced using the HiSeq 2000 platform (Illumina) as paired-end 75 base reads according to manufacturer's protocol. To improve raw alignment BAMs (binary sequence alignments) for SNP calling, we realigned around known (1000 Genomes pilot) indels, and recalibrated base quality scores using GATK (Genome Analysis TookKit; www.broadinstitute.org/gatk/). BAQ (Base Alignment Quality) tags were added using SAMtools (samtools.sourceforge.net/). BAMs were merged to sample level and

duplicates marked using Picard (http://picard.sourceforge.net/). Variants (SNPs and Indels) were called on each sample individually with both SAMtools mpileup (0.1.17) and GATK Unified Genotyper (1.3---21), restricted to exon bait regions plus or minus a 100bp window. Quality filters were applied to each of the callsets separately. Calls were then merged, giving preference to GATK information when possible.

Candidate *de novo* mutations were identified by excluding inherited variants using DeNovoGear (4) http://sourceforge.net/projects/denovogear/). *De novo* calls were annotated with 1000 Genomes allele frequencies, dbSNP132 rsIDs and earliest appearance in dbSNP. Functional annotation was added using Ensembl Variant Effect Predictor v2.2 against Ensembl 64 and included coding consequence predictions, SIFT (5), PolyPhen (6) and Condel annotations (7), Genomic Evolutionary Rate Profiling (http://mendel.stanford.edu/SidowLab/downloads/gerp/index.html) and Grantham Matrix scores.

Variants of interest were prioritised by applying sequence quality filters, excluding minor allele frequencies >0.01 in the 1000 Genomes dataset (http://www.1000genomes.org/home) and limiting the search to coding missense, nonsense, frameshift and essential splice site variants. Variants with low sequencing coverage were removed (number of reads<10). The exome sequencing result was visually inspected using the Integrative Genomics Viewer (8). The functional significance of rare *de novo* variants was predicted by searching the relevant literature on gene function, evolutionary conservation, animal models and gene expression. DNA chromatograms for Sanger sequencing were produced using novoSNP software (9).

Functional studies

Materials

$SYT1_{WT}$-pHluorin and vGLUT1-pHluorin constructs were provided by Prof. V. Haucke (Leibniz Institute of Molecular Pharmacology, Berlin, Germany) and Prof. R. Edwards (University of California, San Francisco, USA) respectively. mCerulean (mCer) empty vector was made as described (10). Neurobasal media, B-27 supplement, penicillin/streptomycin, Minimal Essential Medium (MEM), Lipofectamine 2000 and anti-mouse AlexaFluor 568 were obtained from Invitrogen. Bafilomycin A1 was obtained from Caymen Chemical Company. Mouse anti-synaptotagmin was from Abcam (ab13259). All other reagents were obtained from Sigma-Aldrich.

Plasmid preparation

Site-directed mutagenesis was used to introduce the I368T mutation into the homologous position in rat synaptotagmin (I367) using the forward primer GGACTATGACAAGACTGGCAAGAACGACGCC and reverse primer GGCGTCGTTCTTGCCAGTCTTGTCATAGTCC (mutant bases underlined). The mutation was confirmed by sequencing.

To generate mCer-tagged rat synaptotagmin (mCer-SYT1), mCer was amplified by PCR, with HindIII and AgeI restriction enzyme sites incorporated into the 5' and 3' ends of the mCer sequence respectively, using the forward primer AAGCTTATGGTGAGCAAGGGCGAGGAGC and reverse primer ACCGGTCTTGTACAGCTCGTCCATGCCG (restriction sites underlined). The pHluorin coding sequence of $SYT1_{WT}$-pHluorin was replaced with the PCR transcript by digestion with HindIII and AgeI and ligation into the $SYT1_{WT}$ backbone to create mCer-$SYTI_{WT}$.

Hippocampal neuronal cultures

Dissociated primary hippocampal enriched neuronal cultures were prepared from E17.5 C56BL/6J mouse embryos of both sexes (obtained from an in-house breeding colony) by trituration of isolated hippocampi to obtain a single cell suspension, which was plated at a density of 5 $x10^5$ cells/coverslip

on poly-D-lysine and laminin-coated 25 mm coverslips. Cultures were maintained in neurobasal media supplemented with B-27, 0.5 mM L-glutamine and 1% v/v penicillin/streptomycin. After 72 hours cultures were further supplemented with 1 μM cytosine β-d-arabinofuranoside to inhibit glial proliferation. Cells were transfected after 7 days in culture with Lipofectamine 2000 as described (11). In all experiments 2 constructs were coexpressed; SYT1-pHluorin was cotransfected with mCerulean empty vector (as a transfection marker), while mCer-SYT1 was cotransfected with vGLUT-pHluorin. Cells were imaged after 13-16 days in culture.

Immunolabelling

Immunolabelling of transfected cultured hippocampal neurons was performed as described (11). SYT1-pHluorin was visualized at 480 nm, whereas SYT1 immunolabeling was visualized at 550 nm. Identically sized regions of interest were placed over transfected SYT1 puncta and non-transfected puncta in the same field of view, along with background regions. The level of SYT1 overexpression was calculated by subtracting background autofluorescence prior to ratioing transfected/non-transfected SYT1 expression levels.

Fluorescent imaging protocols

Hippocampal cultures were mounted in a Warner imaging chamber with embedded parallel platinum wires (RC-21BRFS) and placed on the stage of Zeiss Axio Observer D1 epifluorescence microscope. Neurons transfected with mCer vectors were visualised with a Zeiss Plan Apochromat x40 oil immersion objective (NA 1.3) at 430 nm excitation, whereas pHluorin reporters were visualised at 500 nm (both using a dichroic >525 nm and long-pass emission filter, >535 nm). Cultures were stimulated with a train of either 300 or 1200 action potentials delivered at 10 Hz (100 mA, 1 ms pulse width). Cultures were subjected to continuous perfusion with imaging buffer (in mM: 136 NaCl, 2.5 KCl, 2 $CaCl_2$, 1.3 $MgCl_2$, 10 glucose, 10 HEPES, pH 7.4 supplemented with 10 μM 6-cyano-7-nitroquinoxaline-2,3-dione and 50 μM DL-2-Amino-5-phosphonopentanoic acid). To determine exocytosis rate and recycling SV pool size, neurons were stimulated in the presence of bafilomycin A1 (1 μM) to inhibit vesicle acidification. They were then challenged with alkaline imaging buffer

(50 mM NH_4Cl substituted for 50 mM NaCl) to reveal total SYT1-pHluorin fluorescence. Fluorescent images were captured at 4 s intervals using a Hamamatsu Orca-ER digital camera and processed offline using Image J 1.43 software. Regions of interest of identical size were placed over nerve terminals and the total fluorescence intensity was monitored over time. Only regions that responded to action potential stimulation were selected for analysis. All statistical analyses were performed using Microsoft Excel and GraphPad Prism software. The pHluorin fluorescence change was calculated as FΔ/F0, and n refers to the number of individual coverslips examined.

The diffuseness of SYT1-pHluorin fluorescence along axons was determined by calculating the coefficient of variation (CV; as described in (10;12)). The CV for SYT1-pHluorin was calculated following exposure of the cells to alkaline imaging buffer to reveal total SYT1-pHluorin fluorescence. Background autofluorescence (determined by exposure to acidic imaging buffer to quench surface SYT1-pHluorin fluorescence, 20 mM MES substituted for 10 mM HEPES, pH 5.5) was subtracted from image prior to calculating CV. N refers to the mean of 5 different >100 pixel axonal segments on an individual neuron on a single coverslip.

Surface-localised SYT1-pHluorin was determined by exposing transfected neurons to acidic imaging buffer (to quench surface SYT1-pHluorin) followed by standard imaging buffer. Cultures were then exposed to alkaline imaging buffer to reveal total SYT1-pHluorin fluorescence. The surface fraction of SYT1-pHluorin as a percentage of total was calculated using the following equation: [(basal fluorescence - acidic fluorescence)/(alkali fluorescence - acidic fluorescence)] x 100.

References

1. Clarke,A.R., Barry,R.J., McCarthy,R., and Selikowitz,M. Age and sex effects in the EEG: development of the normal child. *Clin. Neurophysiol.* 2001; 112(5):806-814.

2. Cantello,R. et al. Paired-pulse flash-visual evoked potentials: new methods revive an old test. *Clin. Neurophysiol.* 2011; 122(8):1622-1628.

3. Werner,K. et al. Event-related potentials in West syndrome: evidence for bilateral temporal lobe impairment. *Annals of Neurology* 2014.

4. Ramu et al. DeNovoGear: de novo indel and point mutation discovery and phasing. *Nat. Methods* 2013; 10 (10): 985–987.

5. Kumar,P., Henikoff,S., and Ng,P.C. Predicting the effects of coding non-synonymous variants on protein function using the SIFT algorithm. *Nat. Protoc.* 2009; 4(7):1073-1081.

6. Adzhubei,I.A. et al. A method and server for predicting damaging missense mutations. *Nat. Methods* 2010; 7(4):248-249.

7. Gonzalez-Perez,A., and Lopez-Bigas,N. Improving the assessment of the outcome of nonsynonymous SNVs with a consensus deleteriousness score, Condel. *Am. J. Hum. Genet.* 2011; 88(4):440-449.

8. Robinson,J.T. et al. Integrative genomics viewer. *Nat. Biotechnol.* 2011; 29(1):24-26.

9. Weckx,S. et al. novoSNP, a novel computational tool for sequence variation discovery. *Genome Res.* 2005; 15(3):436-442.

10. Gordon,S.L., and Cousin,M.A. X-linked intellectual disability-associated mutations in synaptophysin disrupt synaptobrevin II retrieval. *J. Neurosci.* 2013; 33(34):13695-13700.

11. Gordon,S.L., Leube,R.E., and Cousin,M.A. Synaptophysin is required for synaptobrevin retrieval during synaptic vesicle endocytosis. *J. Neurosci.* 2011; 31(39):14032-14036.

12. Lyles,V., Zhao,Y., and Martin,K.C. Synapse formation and mRNA localization in cultured Aplysia neurons. *Neuron* 2006; 49(3):349-356.

UK 10K Rare Working Group – authors and affiliations

Al-Turki, Saeed [1, 2]
Anderson, Carl [1]
Antony, Dinu [3]
Barroso, Inês [1]
Beales, Phil [3]
Bentham, Jamie [4]
Bhattacharya, Shoumo [4]
Carss, Keren [1]
Chatterjee, Krishna [5]
Cirak, Sebahattin [6]
Cosgrove, Catherine [4]
Danecek, Petr [1]
Durbin, Richard [1]
Fitzpatrick, David [7]
Floyd, Jamie [1]
Foley, A. Reghan [6]
Franklin, Chris [1]
Futema, Marta [8]
Humphries, Steve E. [8]
Hurles, Matt [1]
Joyce, Chris [1]
McCarthy, Shane [1]
Mitchison, Hannah M. [3]
Muddyman, Dawn [1]
Muntoni, Francesco [6]
O'Rahilly, Stephen [5]
Onoufriadis, Alexandros [3]
Payne, Felicity [1]
Plagnol, Vincent [9]
Raymond, Lucy [10]
Savage, David B. [5]
Scambler, Peter [3]
Schmidts, Miriam [3]
Schoenmakers, Nadia [5]
Semple, Robert [5]
Serra, Eva [1]
Stalker, Jim [1]
van Kogelenberg, Margriet [1]
Vijayarangakannan, Parthiban [1]
Walter, Klaudia [1]
Whittall, Ros [8]
Williamson, Kathy [7]

[1] The Wellcome Trust Sanger Institute, Wellcome Trust Genome Campus, Hinxton CB10 1HH, Cambridge, UK.

[2] Department of Pathology, King Abdulaziz Medical City, Riyadh, Saudi Arabia.

[3] Molecular Medicine Unit and Birth Defects Research Centre, UCL Institute of Child Health, London, WC1N 1EH, UK.

[4] Department of Cardiovascular Medicine and Wellcome Trust Centre for Human Genetics, Roosevelt Drive, Oxford, OX3 7BN, UK.

[5] University of Cambridge Metabolic Research Laboratories, and NIHR Cambridge Biomedical Research Centre, Institute of Metabolic Science, Addenbrooke's Hospital, Cambridge, CB2 0QQ, UK.

[6] Dubowitz Neuromuscular Centre, UCL Institute of child health & Great Ormond street Hospital, London, WC1N 3JH, UK.

[7] MRC Human Genetics Unit, MRC Institute of Genetic and Molecular Medicine, at the University of Edinburgh, Western General Hospital, Edinburgh, EH4 2XU, UK.

[8] Cardiovascular Genetics, BHF Laboratories, Rayne Building, Institute Cardiovascular Sciences, University College London, London WC1E 6JJ, UK.

[9] University College London (UCL) Genetics Institute (UGI) Gower Street, London, WC1E 6BT, UK.

[10] Dept. of Medical Genetics, Cambridge Institute for Medical Research, University of Cambridge, CB2 2XY, UK.

[11] Center for Research, Prevention and Treatment of Atherosclerosis, Department of Medicine, Hadassah Hebrew University Medical Center, Jerusalem, Israel.

[12] Department of Biomedical, Metabolic and Neural Sciences, University of Modena and Reggio Emilia, Via campi 287, I-41125 Modena/Italy.

[13] Department of Cardiology, Imperial College Health Services, Charing Cross Hospital, London.